www.elsevier.nl/locate/jorganchem

Journal of Organometallic Chemistry 593–594 (2000) 86–95

Journal of Organometallic Chemistry

The use of macrocyclic and polydentate ligands in ruthenium organometallic chemistry

Christine Stern [a,1], Federico Franceschi [a], Euro Solari [a], Carlo Floriani [a,*], Nazzareno Re [b], Rosario Scopelliti [a]

[a] *Institut de Chimie Minérale et Analytique, BCH, Université de Lausanne, CH-1015 Lausanne, Switzerland*
[b] *Facoltà di Farmacia, Università degli Studi 'G. D'Annunzio', I-66100 Chieti, Italy*

Received 3 May 1999; accepted 16 June 1999

Dedicated to Professor Fausto Calderazzo on the occasion of his 70th birthday.

Abstract

This report deals with two stereochemically different tridentate N_3-ligands suitable as ancillary ligands in the organometallic chemistry of ruthenium. [{Ru(*p*-cymene)(Cl)}$_2$(μ-Cl)$_2$] assisted the template synthesis of a tridentate N_3-macrocycle derived from 2-aminobenzaldehyde, thus forming [Ru(η^3-$C_{21}H_{15}N_3$)Ru(*p*-cymene)]$^{2+}$2Cl$^-$, **1**. The ligand **2**, Pyr–Pic·H, derived from the condensation of pyrrole-2-aldehyde and 2-picolylamine, functions as a monoanionic tridentate ligand in the reaction with [{Ru(COD)(Cl)}$_2$(μ-Cl)$_2$] leading to [Ru(COD)(Cl)(Pyr–Pic–H$_2$)], **4**, which undergoes the ionization of the Ru–Cl bond both in pyridine or in THF in the presence of AgTf, leading to [Ru(Pyr–Pic–H)Py$_3$]$^+$Cl$^-$, **5** and [Ru(COD)(Pyr–Pic–H)Tf], **6**, respectively. The alkylation of **4** using LiMe led to [(Ru–Me)(Pyr–Pic–H)(COD)], **7**, which undergoes a methane elimination to yield [Ru$_2$(μ-Pyr–Pic)$_2$(COD)$_2$], **8**. The reaction of potassium–pyren [pyren = *N*,*N*′-ethylenebis(2-pyrrolyliminato)dianion], **10**, with [{Ru(COD)(Cl)}$_2$(μ-Cl)$_2$] led to the Ru-macrocyclic derivative [Ru(Pyren)(COD)], **11**, where COD fills two *cis*-positions around ruthenium. Extended Hückel calculations have been carried out on the two stereochemically different Ru–N_3 fragments having a facial (see complex **1**) and a meridional (**4**, **5**, **6**, **7** and **8**) arrangements in order to identify the difference in the frontier orbitals for the metal reactivity.

Keywords: Ruthenium; Macrocycle; Template reactions; Pyrrole; Schiff bases

1. Introduction

The use of polydentate or macrocyclic ligands has been so far confined mainly to coordination chemistry, and by far less used as support for organometallic functionalities, except for porphyrin-type derivatives [1] and with Vit. B_{12} models [2]. Much more recently, the use of polydentate ligands, such as Schiff bases [3], dibenzotetramethyltetraaza[14]annulene [4,5], calix-[4]arenes [6], and porphyrinogens [7] have been part of an interesting development in organometallic chemistry. The major focus has been to make available a preorganized set of donor atoms, thus having a metal–ligand fragment with an appropriate set of frontier orbitals

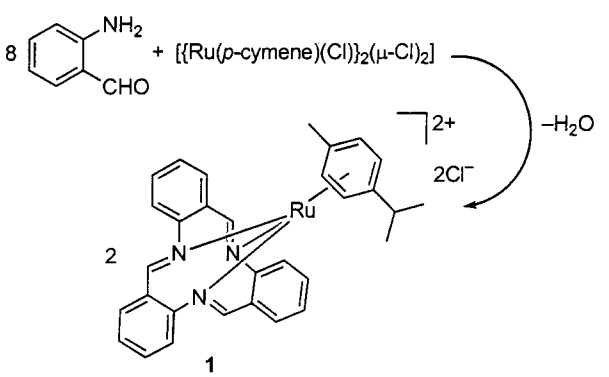

Scheme 1.

* Corresponding author. Fax: +41-21-6923905.
E-mail address: carlo.floriani@icma.unil.ch (C. Floriani)
[1] Present address: Facultés des Sciences Gabriel, LIMSAG, Université de Bourgogne, 6 Boulevard Gabriel, F-21100 Dijon, France.

0022-328X/00/$ - see front matter
PII: S0022-328X(99)00356-3

Table 1
Crystal data and structure refinement for **1**, **5**, **8** and **11**

	1	**5**	**8**	**11**
Formula	$C_{31}H_{29}N_3Ru.5H_2O{\cdot}2Cl$	$C_{26}H_{25}N_6Ru.C_5H_5N{\cdot}Cl$	$C_{38}H_{42}N_6Ru_2$	$C_{20}H_{24}N_4Ru$
Formula weight	705.62	637.14	784.92	421.50
T (K)	143	143	143	143
λ (Å)	0.71069	1.54178	1.54178	1.54178
Crystal system	Orthorombic	Monoclinic	Monoclinic	Monoclinic
Space group	*Pbca*	*I2/a*	*P21/n*	*P21/c*
a (Å)	18.765(3)	18.631(5)	11.982(2)	9.889(4)
b (Å)	16.764(3)	13.823(5)	20.835(3)	19.494(8)
c (Å)	20.084(3)	23.459(7)	13.260(4)	9.111(5)
α (°)	90	90	90	90
β (°)	90	104.84(3)	109.75(3)	93.66(3)
γ (°)	90	90	90	90
V (Å^3)	6318.3(17)	5840(3)	3115.4(12)	1752.8(13)
Z	8	8	4	4
$D_{calc.}$ (g cm^{-3})	1.484	1.449	1.673	1.597
μ (mm^{-1})	0.709	5.446	8.151	7.304
Reflections collected	7256	5520	5579	3423
Data/parameters	7255/411	5396/362	5308/416	3211/227
$R_1[I>2\sigma(I)]$	0.0362	0.0726	0.0374	0.0490
wR_2 (all data)	0.1193	0.2322	0.1166	0.1606

suitable for studying metal-induced activation processes. Such an approach has been poorly pursued in the case of ruthenium, which has a quite remarkable porphyrin-derived chemistry [8]. A limited number of examples deals with the chemical reactivity of [Ru(tmtaa)] [4a,e–f], and Ru–Schiff base fragments [3f–h]. The purpose of the present paper is to describe novel Ru–polydentate complexes, which can be suitable, in perspective, for use in organometallic chemistry. In particular, the use of an N_3 donor set having either a *facial* or *meridional* arrangement around Ru will make available two stereochemically different Ru-fragments for organometallic functionalities. The occurrence of one of them in either a mono- or di-anionic (2-azaallyl) form would affect considerably their reactivity. The extended Hückel calculations allow a qualitative forecast for their difference in reactivity.

2. Results and discussion

2.1. Chemical and structural studies

The [{Ru(*p*-cymene)(Cl)}$_2$(μ-Cl)$_2$] complex drives the *o*-amino benzaldehyde condensation to the formation of the N_3 macrocycle shown in Scheme 1. The metal acts as a particularly appropriate template agent for the trimerization of *o*-aminobenzaldehyde, as expected from the frontier orbitals available for the [Ru–arene]$^{2+}$ fragment (see the following section). We should comment at this stage that the *o*-aminobenzaldehyde self-condensation usually led either to an N_4 or to an N_3 macrocycle, and often to a mixture of both, when solvated metal ions are used [9]. This is, in part, true because the labile solvated metal ions are not really the appropriate template agent for condensing a monomer to the wanted cyclic oligomer. Complex **1** has been fully characterised (see Section 3), including the X-ray analysis.

Crystallographic details are listed in Table 1; selected bond distances and angles in Table 2. The cation shown in Fig. 1 displays a piano-stool geometry (see the structural parameters in Table 2) [Ru–N_{av}, 2.056(4) Å; Ru–(η^6-*p*-cymene)$_{centroid}$, 1.707(4) Å; N–Ru–N_{av}, 82.4(1)°], with ruthenium staying out-of-the N_3 plane by 1.334(2) Å. The folding of the N_3 macrocycle, displaying a pseudo-C_3 symmetry, is shown by the dihedral angle between the arene ring [ring 1: C2, C3, C4, C5, C6, C7; ring 2: C9, C10, C11, C12, C13, C14; ring 3: C16, C17, C18, C19, C20, C21; (1–2), 15.4(2)°; (1–3), 19.7(2)°; (2–3), 25.3(2)°; torsional angles: N1–C1–C2–C7, −27.8(7)°, N3–C15–C16–C21, −25.5(7)°]. The cation in Fig. 1 is held in a polymeric structure by the hydrogen bonding network established between the counteranions Cl^- and the water molecules of crystallization (see supplementary tables and fig. S1).

Preliminary attempts to remove the arene ring from the metal, thus making available the [RuN_3] fragment, using monodentate ligands or via the reduction of the metal have so far been unsuccessful. The [RuN_3] would be a particularly appropriate metal fragment, with a good metal coordinative unsaturation to be used for driving the molecular activation processes. The N_3 macrocycle bonded to ruthenium in complex **1** is forced to fill three coordination sites in a facial mode around

Table 2
Selected bond (Å) and angles (°) for complexes **1**, **5**, **8** and **11**[a]

1					
Ru1–1	2.055(4)	Ru1-η^6(*p*-cymene)	1.707(4)	N=C_{av}	1.281(6)
Ru1–N2	2.059(4)	Ru1-η^3(N3)	1.334(2)	N–C_{av}	1.438(5)
Ru1–N3	2.053(4)	η^3-Ru1-η^6	178.3(1)		
5					
Ru1–N1	2.098(8)	Ru1–N4	2.084(8)	N=C_{av}	1.32(1)
Ru1–N2	2.004(8)	Ru1–N5	2.115(7)	N–C_{av}	1.44(1)
Ru1–N3	2.056(8)	Ru1–N6	2.088(7)		
8					
Ru1–N1	2.169(5)	Ru2–N5	2.035(5)	Ru1-η^2(C23, C24)	2.153(6)
Ru1–N2	2.040(5)	Ru2–N6	2.098(5)	Ru1-η^2(C27, C28)	2.084(6)
Ru1–N3	2.098(5)	Ru1–C17	2.255(6)	Ru2-η^2(C31, C32)	2.087(6)
Ru2–N4	2.169(5)	Ru2–C6	2.252(7)	Ru2-η^2(C35, C36)	2.152(6)
N = C_{av}	1.304(7)	N–C_{av}	1.443(7)		
11					
Ru1–N1	2.086(5)	Ru1–N4	2.090(5)	N=C_{av}	1.303(8)
Ru1–N2	2.087(5)	Ru1-η^2(C13, C14)	2.078(6)	N–C_{av}	1.480(8)
Ru1–N3	2.054(5)	Ru1-η^2(C17, C18)	2.090(6)		

[a] η^2(C, C), η^3(N3), η^6(*p*-cymene) indicate the centroids.

a six-coordinated metal. A different version of a tridentate N_3 ligand has been planned for filling three coordination sites in a meridional plane around a potential octahedral metal. The appropriate ligand has been made by condensing pyrrole-2-aldehyde and 2-picolylamine (see Scheme 2). The resulting ligand, **2**, was deprotonated with BuLi, then reacted in situ with $[\{Ru(COD)(Cl)\}_2(\mu\text{-}Cl)_2]$. The isolation of the lithiated form **3** was not pursued. Complex **4**, which was isolated and fully characterized, has the ligand in a meridional arrangement with COD and Cl filling the remaining coordination sites. The proposed structure has been indirectly proved by the X-ray analysis carried out on **5**, which was obtained by treating **4** with pyridine (Scheme 2). The pyridine replaced COD and ionized the Ru–Cl bond, thus forming a cationic species. The pseudo-octahedral structure of the cation is shown in Fig. 2, while the structural parameters are in Table 2. The tridentate N_3 ligand displays a *meridional* arrangement, while three molecules of pyridine complete the metal coordination sphere (see Table 2). The metal is coplanar [−0.013(4) Å] with the overall ligand, showing the maximum deviation for C10 [0.030(9) Å]. The structural parameters support the proposed bonding scheme (see Scheme 2) for the tridentate ligand.

A different kind of ionization of the Ru–Cl bond was achieved by reacting **4** with $[AgO_3SCF_3]$. In the resulting complex **6**, it has been assumed that the metal maintains the same coordination environment of **4**, with O_3SCF_3 anion replacing Cl^-. The ion-pair formulation is preferred to the ionic form analogous to **5**, because of the high solubility of **6** in hydrocarbon solvents. Complex **4** seems an appropriate starting material for the organic functionalization. Its reaction with LiMe led to a high yield formation of the corresponding methyl derivative **7** (see Section 3). Although the chemistry of the Ru–Me group remains to be explored, we should mention an interesting thermal decomposition pathway, which occurs, however, to a limited extent. The thermally-induced elimination of CH_4 from **7** led to the formation of **8**, via the deprotonation of the methylene group of the ligand **2**. Such an event is driven by the possibility for the ligand to form a bianionic symmetric 2-azaallyl derivative. The monomeric fragment does not survive as such and dimerizes to **8**. The occurrence of the 2-azaallyl formation is monitored by the presence of the CH group in the ^{1}H-NMR spectrum. The 2-azaallyl ligand, though rather rare, has been recently singled out as alkali metal derivatives [10] or complexed to Zr(IV) [11]. The dimeric structure of **8** is shown in Fig. 3.

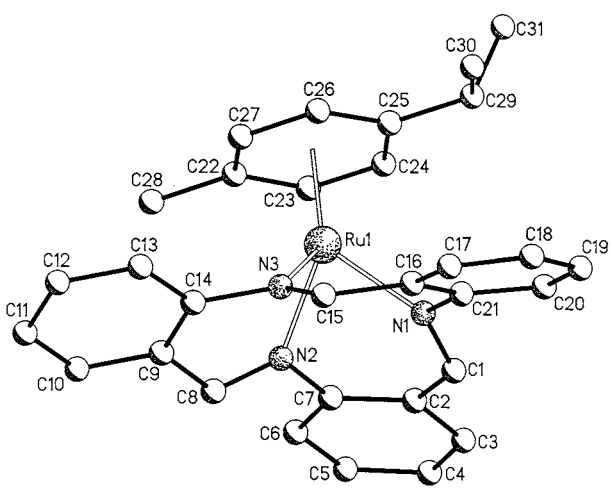

Fig. 1. XP drawing of complex **1**.

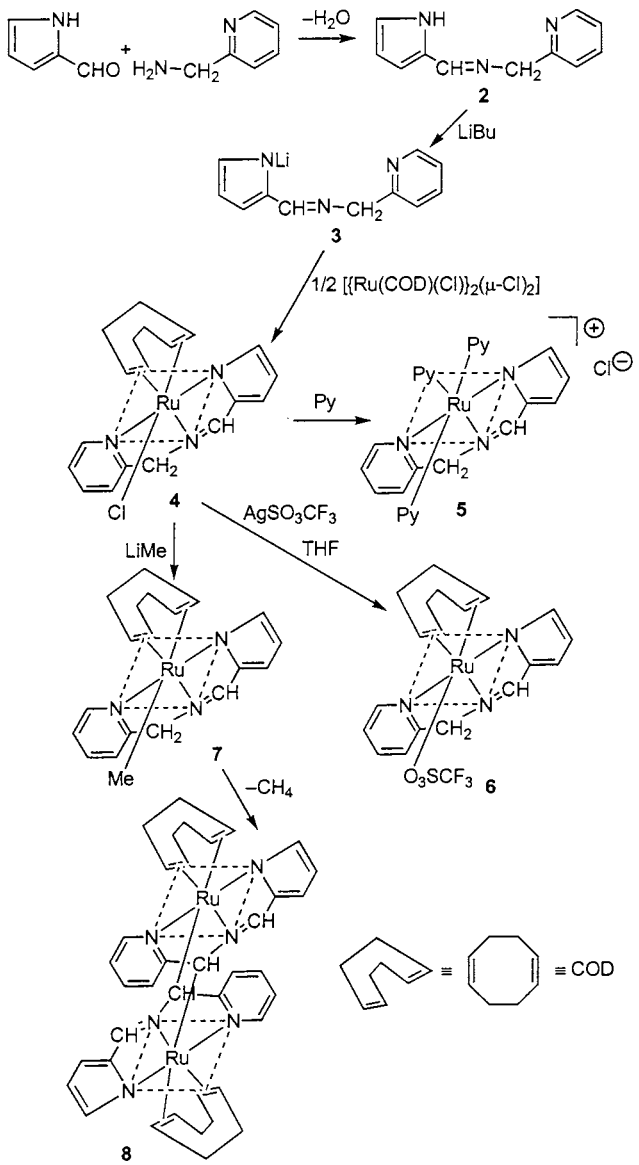

Scheme 2.

The 2-azaallyl form of ligand **3** displays a bridging bonding mode across two ruthenium ions. Each dianionic ligand is η^3-N_3 bonded to one of the ruthenium ions, sharing C6 or C17, respectively, with the other one. The metals complete their coordination sphere bonding COD in an η^4 fashion. Unlike in complex **5**, the deprotonated form of ligand **3** is no longer planar, the torsional angles C7–N2–C6–C5 and C18–N5–C17–C16 being −161.5(6)° and −162.5(6)°, respectively, while the dihedral angles between the pyridine and the pyrrole planes for the ligand around Ru1 and Ru2 are 14.8(3)° and 13.4(4)°, respectively. In addition, the Ru ions are no longer coplanar with the N_3 set of donor atoms [Ru1, −0.125(5); Ru2, 0.132(5) Å]. The bonding sequence for the 2-azaallyl ligand (see Scheme 2) is well supported by the structural data (Table 2). The two alkyl carbons C6 and C17, binding Ru2 and Ru1 respectively, induce a significant lengthening of one of the Ru–(η^2-C=C) bonds of the COD ligand [Ru1–(η^2-C27–C28), 2.084(6); Ru1–(η^2-C23–C24), 2.153(6); Ru2–(η^2-C31–C32), 2.087(6); Ru2–(η^2-C35–C36), 2.152(6) Å], due to the strong *trans*-influence of the carbanionic donor ligand.

Due to the very rich and versatile chemistry of Ru displayed in a macrocyclic environment modelled by the porphyrin [8] or the dibenzotetramethyltetraaza dianions [4a,e–f], we tried, using the same set of donor atoms, to take advantage of the geometrical flexibility of an open chain N_4-tetradentate ligand. This charac-

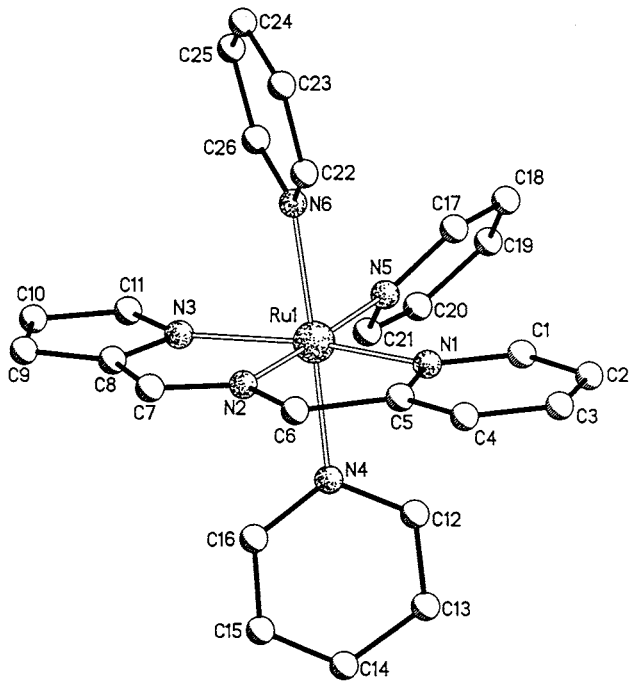

Fig. 2. XP drawing of complex **5**.

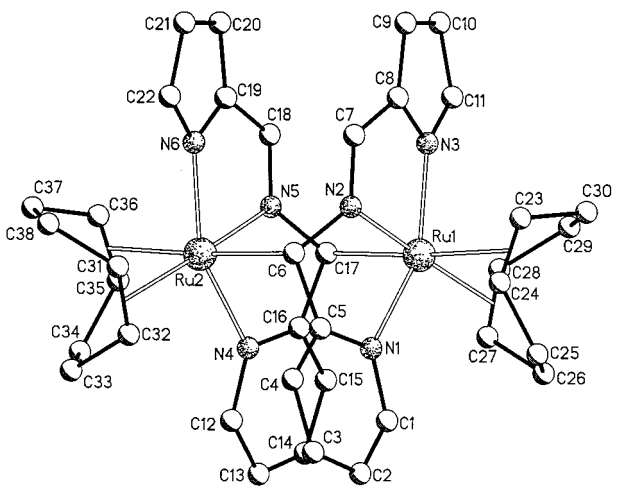

Fig. 3. XP drawing of complex **8**.

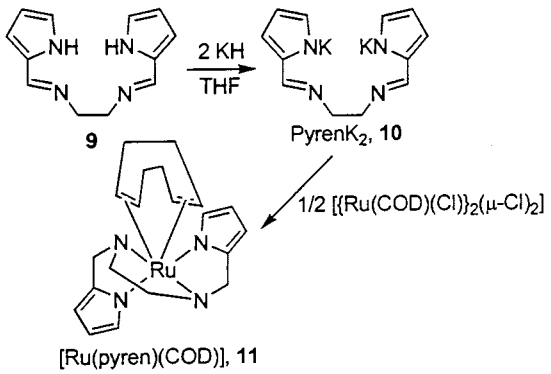

Scheme 3.

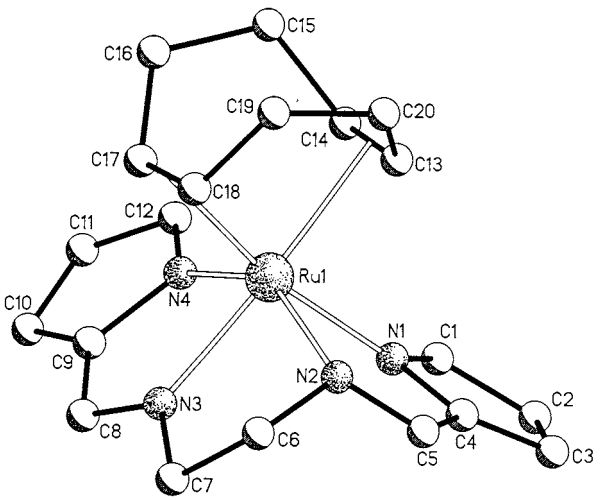

Fig. 4. XP drawing of complex **11**.

teristic would allow the metal to have two additional coordination sites available in a *cis*-arrangement. The ligand of the choice was pyren [pyren = *N*,*N*′-ethylenebis(2-pyrrolyl)iminato dianion], **9** (see Scheme 3). It was transformed into the corresponding K derivative, **10**, then it was metalated using [{Ru(COD)(Cl)}$_2$(μ-Cl)$_2$]. Complex **11** (Fig. 4) has been obtained as a COD adduct. The very high geometrical flexibility is displayed by the quasi-transoid arrangement of the ethylene bridge. This arrangement is unknown in the Schiff base ligands derived from salicylaldehyde [12].

The tetradentate ligand **9** is folded along the C6–C7 bond, the angle between the two pyrrolyl anions being 63.9(3)°, while the torsional angle N2–C6–C7–N3 is −33.1(7)°. The great flexibility of the N_4 tetradentate ligand makes available at the metal two *cis* positions for the COD ligand. The structural parameters for complex **11** are in the expected range.

Complex **11** has a remarkable stability and inertness to the diolefin substitution, at least in the reaction with CO and PR_3.

2.2. Extended Hückel analysis on the [Ru–N_3] complexes

Extended Hückel calculations [13] were performed to elucidate the frontier orbitals of the two [Ru–N_3] fragments having different stereochemistry, one having a facial and the other a meridional arrangement of the three donor atoms.

The molecular orbitals of the facial [Ru(N_3–macrocycle)]$^{2+}$ fragment of **1** have been constructed in a step by step approach. The (N_3-macrocycle) ligand was simplified by replacing the three benzo groups with ethylenes. Next, we considered the planar ligand of D_{3h} symmetry, which was then deformed to reproduce the C_3 geometry of the skeleton in the final complex. The molecular orbitals for the planar ligand are reported in the first column of Fig. 5, while in the second one we illustrate the effect of the bending of the three benzo groups out of the N_3 plane and their torsion with respect to the Ru–N axes. We finally added Ru above the N_3-macrocycle. The resulting MO diagram of this d^6 species is reported in the third column of Fig. 5. Upon coordination, the d orbitals mix strongly with the ligand frontier orbitals, creating five MO's with large metal d character which can be identified. These are the three highest occupied orbitals, i.e. the 1*a*, essentially a d_z2, and the doubly degenerate set 1*e*, constituted mainly by the $d_x2_{-y}2$ and d_{xy} orbitals slightly mixed with d_{xz} and d_{yz} which in the C_3 group belong to the same *e* symmetry. A low-lying 2*e*

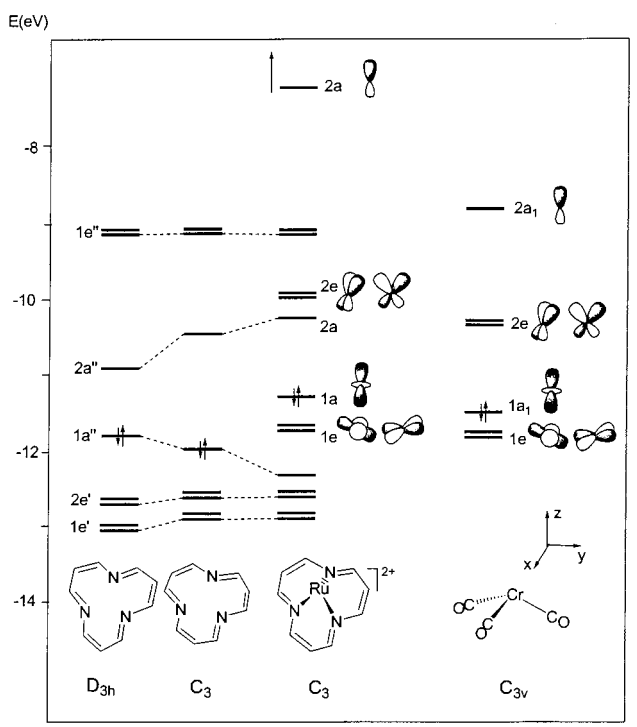

Fig. 5. Building of the frontier MO for [Ru(N_3-macrocycle)]$^{2+}$ and comparison with those for $Cr(CO)_3$.

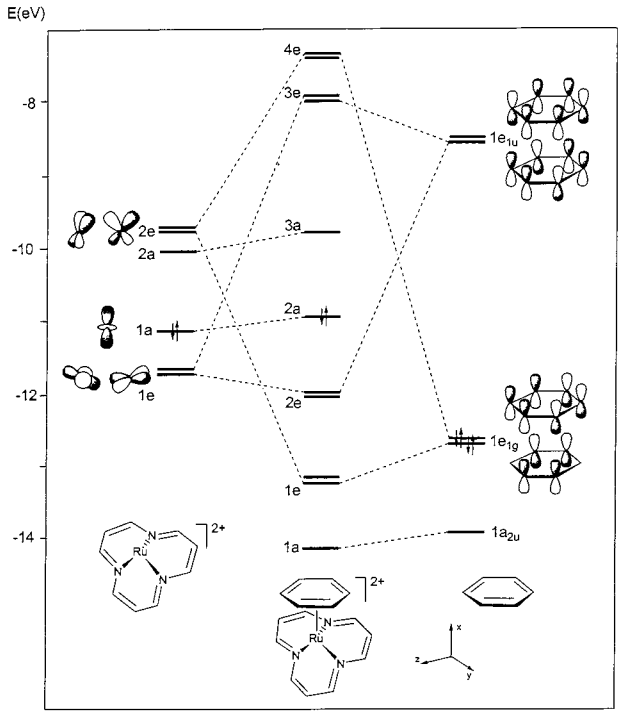

Fig. 6. Orbital correlation diagram for the [Ru(N_3-macrocycle)(C_6H_6)]$^{2+}$.

set is also observed, constituted by d_{xz} and d_{yz} with some $d_{x^2-y^2}$ and d_{xy} character mixed in. Due to their mixing the two sets of orbitals are slightly tilted with respect to the symmetry axis. Such a pattern of frontier orbitals dictate the bonding capabilities and the reactivity of the [Ru(N_3-macrocycle)]$^{2+}$ fragment. In particular, the presence of the high-lying filled 1*e* and the low-lying empty 2*e* set suggest the propensity for interaction with a ligand providing HOMO and LUMO doubly occupied orbitals of proper symmetry. A six electron aromatic cyclic polyene, such as benzene or a cyclopentadienyl anion, is perfectly suited to fulfil these requirements and is therefore expected to bind strongly to the [Ru(N_3-macrocycle)]$^{2+}$ fragment. This is in agreement with the experimental evidence showing that [Ru(N_3-macrocycle)(*p*-cymene)]$^{2+}$ is very stable toward removal of the arene ring. Moreover, the perfect match between the frontier orbitals of [Ru(N_3-macrocycle)] and those of benzene explains why [Ru–arene]$^{2+}$ is a particularly appropriate template agent for the trimerization of *o*-aminobenzaldehyde. The frontier orbital pattern of [Ru(N_3-macrocycle)]$^{2+}$ reminds us to some extent of that for the isoelectronic $M(CO)_3$ fragments[14] such as $Cr(CO)_3$ or $Mn(CO)_3^+$ which form the stable complexes $(CO)_3Cr(C_6H_6)$ and $(CO)_3MnCp$ which have been known since the early stages of organometallic chemistry [15]. The frontier orbitals of the $Cr(CO)_3$ fragment are reported on the right of Fig. 5 and compared with that of [Ru(N_3-macrocycle)]$^{2+}$. We note that the symmetries, the energy ordering and the nodal properties of the metal frontier orbitals for each of the two systems are very similar, thus showing an isolobal analogy [16] between them. The only significant difference between the two fragments consists in the presence in $Cr(CO)_3$ of a low-lying empty orbital of a_1 symmetry (mainly a s–p_z hybrid), which is much higher in energy than that in the [Ru(N_3-macrocycle)]$^{2+}$. The latter is therefore expected to be a poorer electron acceptor. It is also worth noting that the LUMO of [Ru(N_3-macrocycle)]$^{2+}$, 2*a*, is essentially a non bonding π orbital of the ligand mainly localized on the iminato carbons, making these atoms susceptible to a nucleophilic attack. Although the reactivity of **1** toward nucleophilic species has not yet been investigated, our calculations suggest the same regiochemistry observed for analogous N_3- and N_4-macrocycle complexes which undergo nucleophilic attack on the iminato carbons [12].

We then considered the bonding between the aromatic ring and the metal fragment in **1**, replacing the *p*-cymene ligand with benzene which allowed us to maintain the C_3 symmetry. An orbital correlation diagram for the [Ru(N_3-macrocycle)(C_6H_6)]$^{2+}$ in terms of its constituent fragments [Ru(N_3-macrocycle)]$^{2+}$ and C_6H_6 is shown in Fig. 6. On the left of Fig. 6 we report the frontier orbital of the metal fragment discussed above while on the right there are the main frontier orbitals of C_6H_6, i.e. the $1a_{2u}(\pi_o)$, the $1e_{1g}(\pi_1)$ and $1e_{1u}(\pi_2)$ with none, one and two nodes, respectively. The degenerate π_1 set of benzene is considerably stabilized by the empty 2*e* set on the metal fragment, yielding the bonding and antibonding combinations 1*e* and 2*e*. Fig. 6 also shows a significant interaction between the empty π_2 of benzene and the filled metal 1*e* orbital. However the latter is a δ-type interaction and is expected to be weaker than the previous π-type interaction π_1–2*e* (see Scheme 2), as evidenced by the lower population calculated in the complex for the π_2 (0.15) to that of 1*e* (0.25). The ruthenium–benzene interaction leads, therefore, to a net electron density transfer from the aromatic ring to the metal, as evidenced by a Mulliken population analysis of the complex, indicating a charge of $+0.4$ *e* on the benzene unit, and suggests a possible activation of the arene ring toward nucleophilic substitution.

The following analysis focuses on the [Ru(N_3-ligand)]$^+$ fragment present in complexes **4**–**8**. The three N donor atoms have in these cases a meridional arrangement. Once again, a step by step approach was used to build appropriate molecular orbitals. The molecular orbitals for the planar N_3-ligand are reported in the first column of Fig. 7, while in the second one we illustrate the final MO's diagram after the addition of the ruthenium atom. After coordination, five MO with large metal d character can be identified. Four of them are almost degenerate, within 0.2 eV, in increasing

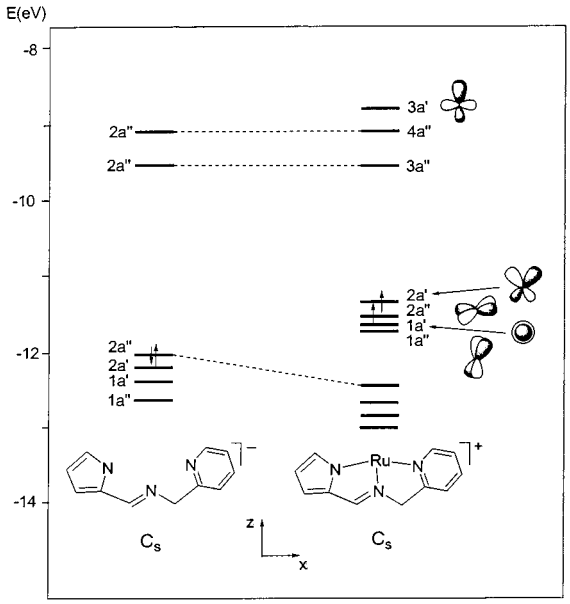

Fig. 7. Building of the frontier MO for $[Ru(N_3\text{-ligand})]^+$.

energy order, $1a''(d_{yz})$, $1a'(d_y2)$, $2a'(d_{xz})$ and $2a''(d_{xy})$ where the (d_{xy}) and (d_{xz}) belonging to the same a'' symmetry are significantly mixed and tilted out of the yz and xy planes. A further metal orbital, $3a'(d_x2_{-z}2)$, pointing in the N_3 ligand plane, but hybridized toward the z direction, lies much higher in energy. The bonding capabilities and the reactivity of the $[Ru(N_3\text{-ligand})]^+$ fragment are dictated by these frontier orbitals. This fragment could easily bind three σ ligands in a *meridional* arrangement restoring a stable pseudo-octahedral coordination as observed in **5**. The presence of the three π-donor orthogonal orbitals suggests the optimal stabilization of up to two olefins in the *cis* position, as observed in **4**. It is also worth noting the presence of a low-energy LUMO, $3a''$, corresponding closely to the LUMO of the N_3-ligand, which is a π* orbital mainly localized on the iminato carbon atom making it susceptible to a nucleophilic attack.

3. Experimental

3.1. General procedures

All operations were carried out under an atmosphere of purified nitrogen. All solvents were purified by standard methods and freshly distilled prior to use. Infrared spectra were recorded with a Perkin-Elmer FT 1600 spectrophotometer, NMR spectra were recorded on AC-200 and DPX-400 Bruker spectrometers. $[\{Ru(COD)(Cl)\}_2(\mu\text{-}Cl)_2]$ [17], $[\{Ru(p\text{-cymene})(Cl)\}_2(\mu\text{-}Cl)_2]$ [18], *o*-aminobenzaldehyde [19] and $pyrenH_2$ [20] were prepared according to published procedures. All the extended Hückel calculations were performed with the program CACAO (computer aided composition of atomic orbitals) [21] using standard atomic parameters [22].

3.2. Synthesis of **1**

$[\{Ru(p\text{-cymene})(Cl)\}_2(\mu\text{-}Cl)_2]$ (2.78 g, 4.54 mmol) was added to an ethanol (200 ml) solution of *o*-aminobenzaldehyde (4.40 g, 36.3 mmol) and this mixture was refluxed overnight. The solution was taken to dryness, and the residue was stirred in *n*-hexane (150 ml) and stirred for 30 min. The green solid was collected and dried in vacuo (4.92 g; 88%). Crystals suitable for X-ray analysis were grown in CH_2Cl_2. (Found: C, 60.56; H, 4.81. $C_{31}H_{29}Cl_2N_3Ru$ requires C, 60.49; H, 4.75; N, 6.83%). ^{1}H-NMR (CD_3OD, 200 MHz, 298 K): δ 8.93 (s, 3H, CH=N); 8.08 (m, 9H, Ar TRI); 7.81 (m, 3H, Ar TRI); 5.76 (m, 2H, Ar *p*-cy); 5.64 (m, 2H, Ar *p*-cy); 2.38 (m, 1H, CH *p*-cy); 1.78 (s, 3H, CH_3 *p*-cy); 0.89 (d, $J = 6.8$ Hz, 3H, CH_3 *p*-cy); 0.78 (d, $J = 6.8$ Hz, 3H, CH_3 *p*-cy). IR (nujol, ν_{max}/cm^{-1}): 1607(s), 1590(s), 1565(s), 1307(m), 1244(m), 1187(m), 1044(m), 970(w), 883(w), 783(s), 523(m).

3.3. Synthesis of **2**

Pyrrole-2-carboxaldehyde (10.69 g, 112.26 mmol) and 2-picolylamine (11.50 ml, 112.26 mmol) were dissolved in CH_2Cl_2 (150 ml). The resulting solution was stirred overnight at room temperature and then filtered. The solvent was evaporated to dryness and the suspension in *n*-hexane (200 ml) of the residue was stirred for 30 min. The product was then collected and dried in vacuo (19.13 g, 92%). ^{1}H-NMR ($CDCl_3$, 400 MHz, 298 K): δ 8.48 (d, $J = 4.8$ Hz, 1H, CH py); 8.16 (s, 1H, CH=N); 7.46 (m, 1H, CH py); 7.19 (d, $J = 7.6$ Hz, 1H, CH py); 7.04 (m, 1H, CH py); 6.66 (d, $J = 1.2$ Hz, 1H, CH pyr); 6.47 (m, 1H, CH pyr), 6.12 (m, 1H, CH pyr); 4.82 (s, 2H, CH_2). ^{13}C-NMR ($CDCl_3$, 100.6 MHz, 298 K): δ 159.3 (C_{quat} py); 154.0 (CH=N); 149.0 (CH py); 136.4 (CH py); 129.8 (C_{quat} pyr); 122.3 (CH py); 121.9 (CH py); 121.7 (CH pyr); 115.1 (CH pyr); 109.5 (CH pyr); 65.9 (CH_2). IR (nujol, ν_{max}/cm^{-1}): 1627(s), 1592(s), 1418(s), 1303(m), 1131(m), 1092(w), 1016(w), 1002(m), 880(w), 789(m), 736(s), 632(w), 607(m), 520(w).

3.4. Synthesis of **4**

Butyllithium (33.60 mmol, 1.60M in *n*-hexane) was added dropwise to **2** (5.96 g, 32.18 mmol) dissolved in THF (500 ml). This solution was continuously stirred for 3 h, then $[\{Ru(COD)(Cl)\}_2(\mu\text{-}Cl)_2]$ (9.02 g, 16.9 mmol) was added and the mixture was stirred overnight. The product precipitated as a green solid which was collected and dried in vacuo (7.05 g, 51%). (Found: C, 53.13; H, 5.25; N, 9.69. $C_{19}H_{22}ClN_3Ru$

requires C, 53.20; H, 5.17; N, 9.79%). ^{1}H-NMR (pyridine-d_5, 400 MHz, 298 K): δ 9.39 (d, $J = 6.8$ Hz, 1H, CH py); 8.01 (s, 1H, CH=N); 7.73 (br s, 1H, pyr); 7.66 (t, $J = 7.8$ Hz, 1H, py); 7.37 (t, $J = 6.8$ Hz, 1H, py); 7.29 (d, $J = 7.8$ Hz, 1H, py); 7.08 (m, 1H, pyr); 6.62 (m, 1H, pyr); 5.27 (d, $J = 20.0$ Hz, 1H, CH_2); 5.15 (d, $J = 20.0$ Hz, 1H, CH_2); 5.08 (m, 1H, CH COD); 4.69 (m, 1H, CH COD); 3.45 (m, 1H, CH COD); 2.82 (m, 1H, CH COD); 2.59 (m, 2H, CH_2 COD); 2.26 (m, 1H, CH_2 COD); 2.14 (m, 1H, CH_2 COD); 2.01 (m, 2H, CH_2 COD); 1.79 (m, 2H, CH_2 COD). ^{13}C-NMR (pyridine-d_5, 100.6 MHz, 298 K): δ 164.3 (C_{quat} py); 155.0 (CH=N); 154.3 (CH py); 142.9 (C_{quat} pyr); 137.8 (CH py); 136.6 (CH pyr); 124.4 (CH py); 121.5 (CH pyr); 116.6 (CH pyr); 111.5 (CH pyr); 92.1 (CH COD); 91.4 (CH COD); 89.8 (CH COD); 82.0 (CH COD); 61.6 (CH_2); 31.6 (CH_2 COD); 30.6 (CH_2 COD); 29.6 (CH_2 COD); 28.7 (CH_2 COD). IR (nujol, ν_{max}/cm^{-1}): 1709(w), 1650(w), 1609(s), 1591(s), 1518(s), 1391(m), 1375(m), 1355(m), 1330(m), 1303(s), 1285(m), 1262(w), 1212(w), 1189(w), 1159(w), 1086(m), 1062(w), 1033(s), 983(m), 930(w), 875(w), 832(m), 775(m), 754(s), 728(s), 682(s), 651(m), 613(m), 543(s), 496(w), 455(s), 440(m).

3.5. Synthesis of **5**

Complex **4** (3.15 g, 7.34 mmol) was extracted in hot pyridine (60 ml). The mixture was refluxed for 4 h, then concentrated to 20 ml. *n*-Hexane (200 ml) was added and a brown microcrystalline product was collected and dried in vacuo (2.69 g, 55%). Recrystallisation from a mixture of pyridine and heptane gave crystals suitable for X-ray analysis. (Found: C, 61.21; H, 5.78; N, 12.36. $C_{34}H_{37}ClN_6Ru$ requires C, 61.30; H, 5.60; N, 12.61%).

3.6. Synthesis of **6**

$AgSO_3CF_3$ (1.35 g, 5.25 mmol) was added to a THF (300 ml) suspension of **4** (2.25 g, 5.25 mmol). Aluminium foil was used to protect the reaction flask from light. The mixture was stirred for 3 h and then refluxed overnight. After removing AgCl by filtration, the red solution was taken to dryness. The remaining residue, suspended and stirred in *n*-hexane (200 ml), gave a green solid, which was collected and dried in vacuo (2.33 g, 82%). (Found: C, 44.12; H, 3.99; N, 7.41. $C_{20}H_{22}F_3N_3O_3RuS$ requires C, 44.28; H, 4.09; N, 7.75%). ^{1}H-NMR (pyridine-d_5, 400 MHz, 298 K): δ 9.31 (d, $J = 6.3$ Hz, 1H, CH py); 8.35 (s, 1H, CH=N); 7.90 (t, $J = 7.8$ Hz, 1H py); 7.68 (d, $J = 7.8$ Hz, 1H py); 7.55 (t, $J = 6.3$ Hz, 1H, pyridine); 7.50 (br s, 1H, pyr); 7.10 (d, $J = 3.9$ Hz, 1H, pyr); 6.50 (m, 1H, pyr); 5.76 (d, $J = 20.8$ Hz, 1H, CH_2); 5.64 (d, $J = 20.8$ Hz, 1H, CH_2); 4.79 (m, 1H, CH COD); 4.68 (m, 1H, CH COD); 3.78 (m, 1H, CH COD); 3.22 (m, 1H, CH COD); 2.78 (m, 1H, CH_2 COD); 2.64 (m, 1H, CH_2 COD); 2.34 (m, 1H, CH_2 COD); 2.15 (m, 1H, CH_2 COD); 1.96 (m, 3H, CH_2 COD); 1.82 (m, 1H, CH_2 COD). ^{13}C-NMR (pyridine-d_5, 100.6 MHz, 298 K): δ 164.9 (C_{quat} py); 157.1 (CH=N); 153.9 (CH py); 142.7 (C_{quat} pyr); 139.4 (CH py); 137.5 (CH pyr); 125.7 (CH py); 123.4 (CH py); 119.4 (CH pyr); 113.2 (CH pyr); 95.1 (CH COD); 91.8 (CH COD); 90.9 (CH COD); 88.6 (CH COD); 61.4 (CH_2); 30.4 (CH_2 COD); 29.8 (CH_2 COD); 29.6 (CH_2 COD); 28.3 (CH_2 COD).

3.7. Synthesis of **7**

Methyllithium (9.73 mmol, 1.65M in Et_2O) was added dropwise to a toluene (400 ml) suspension of **4** (4.20 g, 9.79 mmol) cooled previously at -30°C. The mixture was allowed to reach room temperature and stirred overnight. LiCl was filtered off and the dark-green solution was taken to dryness. A suspension of the green residue was made in *n*-hexane (100 mL), stirred for 15 min, then collected and dried in vacuo (3.37 g, 84%). (Found: C, 58.58; H, 5.97; N, 9.95. $C_{20}H_{26}N_3Ru$ requires C, 58.66; H, 6.40; N, 10.26%). ^{1}H-NMR (pyridine-d_5, 400 MHz, 298 K): δ 8.84 (d, $J = 5.4$ Hz, 1H, CH py); 8.04 (d, $J = 1.0$ Hz, 1H, CH=N); 7.57 (td, $J = 7.8$ Hz, $J = 1.5$ Hz, 1H py); 7.49 (br s, 1H, CH pyr); 7.22 (m, 2H, CH py); 7.04 (m, 1H, CH pyr); 6.65 (m, 1H, CH pyr); 5.26 (d, $J = 19.6$ Hz, 1H, CH_2); 5.09 (d, $J = 19.6$ Hz, 1H, CH_2); 4.12 (m, 1H, CH COD); 4.03 (m, 1H, CH COD); 3.43 (m, 1H, CH COD); 3.29 (m, 1H, CH COD); 2.73 (m, 1H, CH_2 COD); 2.62 (m, 1H, CH_2 COD); 2.57 (m, 1H, CH_2 COD); 2.26 (m, 1H, CH_2 COD); 2.08 (m, 2H, CH_2 COD); 1.93 (m, 1H, CH_2 COD); 1.79 (m, 1H, CH_2 COD); -0.19 (s, 3H, CH_3). ^{13}C-NMR (pyridine-d_5, 100.6 MHz, 298 K): δ 163.5 (C_{quat} py); 152.9 (CH py); 150.2 (CH=N); 142.5 (C_{quat} pyr); 136.0 (CH py); 135.1 (CH pyr); 124.2 (CH py); 120.7 (CH py); 113.8 (CH pyr); 110.8 (CH pyr); 99.5 (CH COD); 91.9 (CH COD); 84.8 (CH COD); 83.9 (CH COD); 62.2 (CH_2); 32.2 (CH_2 COD); 31.8 (CH_2 COD); 30.1 (CH_2 COD); 29.0 (CH_2 COD); 11.4 (CH_3).

3.8. Synthesis of **8**

This compound can be obtained in modest yield as a decomposition product of **7**. During the reaction work-up, after LiCl has been filtered off, if one allows the solution to stand at room temperature for 48 h, **8** can be collected as a red microcrystalline product (0.2 g, 7% starting from 3.25 g of **4** in 400 ml of toluene). Crystals suitable for X-ray analysis were obtained from the mother liquor. (Found: C, 57.81; H, 5.39; N, 10.55. $C_{19}H_{21}N_3Ru$ requires C, 58.15; H, 5.39; N, 10.71%). ^{1}H-NMR (CD_2Cl_2, 400 MHz, 298 K): δ 7.61 (dd, $J = 1.5$ Hz, $J = 7.0$ Hz, 1H, CH py); 7.39 (ddd, $J = 1.5$ Hz, $J = 7.0$ Hz, $J = 8.0$ Hz, 1H, CH py); 7.31 (br s, 1H,

CH pyr); 6.42 (dd, $J = 1.5$ Hz, $J = 8.0$ Hz, 1H, CH py); 6.35 (dd, $J = 1.7$ Hz, $J = 3.7$ Hz, 1H, CH pyr); 6.33 (ddd, $J = 1.5$ Hz, $J = 7.0$ Hz, $J = 8.0$ Hz, 1H, CH py); 6.12 (dd, $J = 1.7$ Hz, $J = 3.7$ Hz, 1H, CH pyr); 5.31 (s, 1H, CH–N); 5.00 (s, 1H, CH–N); 4.45 (m, 1H, COD); 3.14 (m, 2H, COD); 2.95 (m, 2H, COD); 2.34 (m, 2H, COD); 1.81 (m, 2H, COD); 1.67 (m, 1H, COD); 1.56 (m, 1H, COD); 1.48 (m, 1H, COD).

3.9. Synthesis of **10**

KH (6.21 g, 154.9 mmol) was slowly added to a THF (1 l) solution of pyrenH_2 (16.6 g, 77.4 mmol) and this suspension was refluxed overnight. The white solid was collected and dried in vacuo (21.15 g, 94%). (Found: C, 49.72; H, 4.00; N, 19.19. $C_{12}H_{12}K_2N_4$ requires C, 49.62; H, 4.16; N, 19.29%). ^{1}H-NMR (DMSO-d_6, 400 MHz, 298 K): δ 7.95 (s, 2H, CH=N); 6.73 (s, 2H, CH); 6.24 (m, 2H, CH); 5.83 (m, 2H, CH); 3.47 (s, 4H, CH_2). ^{13}C-NMR (DMSO-d_6, 100.6 MHz, 298 K): δ 158.5 (CH=N); 138.4 (C_{quat}); 133.2 (CH); 113.1 (CH); 107.3 (CH); 63.2 (CH_2).

3.10. Synthesis of **11**

[{Ru(COD)(Cl)}$_2$(μ-Cl)$_2$] (6.0 g, 10.7 mmol) was added to a THF (350 ml) suspension of **10** (6.22 g, 21.4 mmol). The mixture was refluxed overnight, after which time KCl was filtered off and the solution taken to dryness. An *n*-hexane (200 ml) suspension of the residue was stirred for 30 min, resulting in a brown solid, which was collected and dried in vacuo (6.05 g, 67%). Crystals suitable for X-ray analysis were grown in a toluene solution. (Found: C, 56.33; H, 5.78; N, 13.15. $C_{20}H_{24}N_4Ru$ requires C, 56.99; H, 5.74; N, 13.29%). ^{1}H-NMR (pyridine-d_5, 400 MHz, 298 K): δ 8.13 (s, 1H, CH=N); 7.73 (s, 1H, CH=N); 7.53 (s, 1H, CH pyr); 7.02 (s, 1H, CH pyr); 6.99 (d, $J = 3.9$ Hz, 1H, CH pyr); 6.91 (d, $J = 3.9$ Hz, 1H, CH pyr); 6.73 (m, 1H, CH pyr); 6.27 (m, 1H, CH pyr); 4.67 (m, 1H, CH COD); 4.10 (m, 1H, CH COD); 4.06 (m, 2H, CH_2); 3.75 (m, 1H, CH COD); 3.66 (m, 2H, CH_2); 3.46 (m, 1H, CH COD); 2.90 (m, 1H, CH_2 COD); 2.48 (m, 2H, CH_2 COD); 2.26 (m, 3H, CH_2 COD); 1.96 (m, 2H, CH_2 COD). ^{13}C-NMR (pyridine-d_5, 100.6 MHz, 298 K): δ 162.5 (CH=N); 154.9 (CH=N); 144.1 (C_{quat} pyr); 140.7 (C_{quat} pyr); 136.4 (CH pyr); 135.0 (CH pyr); 116.1 (CH pyr); 115.6 (CH pyr); 113.5 (CH pyr); 111.6 (CH pyr); 93.3 (CH COD); 87.0 (CH COD); 83.5 (CH COD); 81.9 (CH COD); 62.5 (CH_2); 57.5 (CH_2); 32.9 (CH_2 COD); 32.5 (CH_2 COD); 29.8 (CH_2 COD); 28.6 (CH_2 COD). IR (nujol, ν_{max}/cm^{-1}): 1634(m), 1584(s), 1567(s), 1389(s), 1317(s), 1300(s), 1217(w), 1195(w), 1089(w), 1033(s), 933(w), 778(w), 728(w), 678(w), 611(w).

3.11. X-ray experimental section

Crystallographic details are listed in Table 1. Suitable crystals for X-ray diffraction were mounted on glass capillaries and sealed under nitrogen. Diffraction data were collected on Rigaku AFC6S (**5**, **8**, **11**) and AFC7S (**1**) four-circle diffractometers at 143 K and then processed with teXsan [23]. Structure solutions were performed by direct methods with the program SHELXS 97 [24]. The refinements were carried out by full-matrix-block least squares on F^2 with all non-H atoms refined anisotropically using the program SHELXL-97-2 PC version [25]. H atoms were calculated on idealized positions and their isotropic displacement parameters were fixed to a^*U_{eq}(C) (where a is 1.5 for methyl hydrogens and 1.2 for others and C is the parent carbon atom) except those belonging to the pyridine molecule in compound **5** for which a unique U_{iso} (0.08 Å^2) was applied. Molecular graphics by XP [26]. Material for publication and geometrical calculations have been prepared with XCIF included in the SHELXTL software package [27] and SHELXL-97-2 PC version, respectively.

4. Supplementary information

Crystallographic data (excluding structure factors) for the structures reported in this paper have been deposited with the Cambridge Crystallographic Data Centre as supplementary publication no. CCDC-125999 for **1**, CCDC-126000 for **5**, CCDC-126001 for **8**, and CCDC-126002 for **11**. Copies of the data can be obtained free of charge on application to CCDC, 12 Union Road, Cambridge CB2 1EZ, UK (Fax: +44-1223-336033; E-mail: deposit@ ccdc.cam.ac.uk; http://www.ccdc.cam.ac.uk).

Fig. S1, tables giving crystal data and structure refinement, atomic coordinates, bond length and angles, anisotropic displacement parameters, hydrogen coordinates and isotropic displacement parameters, and torsion angles for **1**, **5**, **8**, and **11** (pp. 29).

Acknowledgements

We thank the 'Fonds National Suisse de la Recherche Scientifique' (Bern, Switzerland, Grant No. 20-53336.98) and Action COST D9 (European Program for Scientific Research, OFES No. C98.008) for financial support.

References

[1] (a) K.M. Smith (Ed.), Porphyrins and Metalloporphyrins, Elsevier, Amsterdam, 1975. (b) D. Dolphin (Ed.), The Porphyrins, Academic, New York, 1978.

[2] (a) R.L. Sweany, in: E.W. Abel, F.G.A. Stone, G. Wilkinson (Eds.), Comprehensive Organometallic Chemistry II, vol. 8, Pergamon, Oxford, 1995, pp. 42 (Chapter 1) and references therein. (b) M. Calligaris, L. Randaccio, in: G. Wilkinson, R.D. Gillard, J.A. McCleverty (Eds.), Comprehensive Coordination Chemistry, Pergamon, Oxford, 1987. (c) J.M. Pratt, P.J. Craig, Adv. Organomet. Chem. 11 (1973) 404. (d) M. Calligaris, G. Nardin, L. Randaccio, Coord. Chem. Rev. 7 (1972) 385. (e) A. Bigotto, G. Costa, G. Mestroni, G. Pellizzer, A. Puxeddu, E. Reisenhofer, L. Stefani, G. Tauzher, Inorg. Chim. Acta 4 (1970) 41. (f) G. Pattenden, Chem. Soc. Rev. 17 (1988) 361 and references therein. (g) D. Dodd, M.D. Johnson, J. Organomet. Chem. 52 (1973) 1. (h) J.M. Pratt, P.J. Craig, Adv. Organomet. Chem. 11 (1973) 414. (i) L. Randaccio, N. Bresciani-Pahor, E. Zangrando, L.G. Marzilli, Chem. Soc. Rev. 18 (1989) 225. (j) J.-P. Charlaud, E. Zangrando, N. Bresciani-Pahor, L. Randaccio, L.G. Marzilli, Inorg. Chem. 32 (1993) 4256.

[3] (a) C. Floriani, E. Solari, F. Corazza, A. Chiesi-Villa, C. Guastini, Angew. Chem. Int. Ed. Engl. 28 (1989) 64. (b) J.M. Rosset, C. Floriani, M. Mazzanti, A. Chiesi-Villa, C. Guastini, Inorg. Chem. 29 (1990) 3991. (c) E. Solari, C. Floriani, A. Chiesi-Villa, C. Rizzoli, J. Chem. Soc. Dalton Trans. (1992) 367. (d) E.B. Tjaden, D.C. Swenson, R.F. Jordan, J.L. Petersen, Organometallics 14 (1995) 371. (e) E. Gallo, E. Solari, C. Floriani, A. Chiesi-Villa, C. Rizzoli, Inorg. Chem. 36 (1997) 2178. (f) H. Brunner, R. Oeschey, B. Nuber, J. Chem. Soc. Dalton Trans. (1996) 1499. (g) K. Ghosh, S. Pattanayak, A. Chakravorty, Organometallics 17 (1998) 1956. (h) S. Chang, L. Jones II, C. Wang, L.M. Henling, R.H. Grubbs, Organometallics 17 (1998) 3460.

[4] (a) F.A. Cotton, J. Czuchajowska, Polyhedron 9 (1990) 1221. (b) L. Giannini, E. Solari, C. Floriani, A. Chiesi-Villa, C. Rizzoli, Angew. Chem. Int. Ed. Engl. 33 (1994) 2204. (c) L. Giannini, E. Solari, S. De Angelis, T.R. Ward, C. Floriani, A. Chiesi-Villa, C. Rizzoli, J. Am. Chem. Soc. 117 (1995) 5801. (d) D.G. Black, D.C. Swenson, R.F. Jordan, R.D. Rogers, Organometallics 14 (1995) 3539. (e) A. Klose, E. Solari, C. Floriani, S. Geremia, L. Randaccio, Angew. Chem. Int. Ed. Engl. 37 (1998) 148. (f) A. Klose, E. Solari, J. Hesschenbrouck, C. Floriani, N. Re, S. Geremia, L. Randaccio, Organometallics 18 (1999) 360.

[5] (a) F.A. Cotton, J. Czuchajowska, Polyhedron 9 (1990) 2553. (b) P. Mountford, Chem. Soc. Rev. 27 (1998) 105.

[6] C. Floriani, Chem. Eur. J. 5 (1999) 19 and references therein.

[7] C. Floriani, Pure Appl. Chem. 68 (1996) 1 and references therein.

[8] (a) J.P. Collman, C.E. Barnes, P.N. Swepston, J.A. Ibers, J. Am. Chem. Soc. 106 (1984) 3500. (b) J.P. Collman, P.J. Brothers, L. Mc Elwee-White, E. Rose, L.J. Wright, J. Am. Chem. Soc. 107 (1985) 4570. (c) J.P. Collman, P.J. Brothers, L. Mc Elwee-White, E. Rose, J. Am. Chem. Soc. 107 (1985) 6110. (d) D.R. Casimiro, D.N. Beratan, J.N. Onuchic, J.R. Winkler, H.B. Gray, Adv. Chem. Ser. 246 (1995) 471. (e) R. Salzmann, C.J. Ziegler, N. Godbout, M.T. McMahon, K.S. Suslick, E. Oldfield, J. Am. Chem. Soc. 120 (1998) 11323. (f) R. Zhang, W.-Y. Yu, T.-S. Lai, C.-M. Che, Chem. Commun. (1999) 409.

[9] A.G. Kolchinski, Coord. Chem. Rev. 174 (1998) 207.

[10] P.C. Andrews, D.R. Armstrong, W. Clegg, F.J. Craig, L. Dunbar, R.E. Mulvey, Chem. Commun. (1997) 319.

[11] P. Veya, C. Floriani, A. Chiesi-Villa, C. Guastini, J. Chem. Soc. Chem. Commun. (1991) 991.

[12] M. Calligaris, L. Randaccio, in: G. Wilkinson, R.D. Gillard, J.A. McLaverty (Eds.), Comprehensive Coordination Chemistry, vol. 2, Pergamon, Oxford, UK, 1987 (Chapter 20.1).

[13] (a) R. Hoffmann, W.N. Lipscomb, J. Chem. Phys. 36 (1962) 2179. (b) R. Hoffmann, J. Chem. Phys. 39 (1963) 1397.

[14] M. Elian, R. Hoffmann, Inorg. Chem. 14 (1975) 1058.

[15] (a) E.O. Fischer, K. Ofele, Chem. Ber. 90 (1957) 2532. (b) E.O. Fischer, R. Jira, Z. Naturforsch. 9 (1954) 618.

[16] (a) R. Hoffmann, Angew. Chem. Int. Ed. Engl. 21 (1982) 711. (b) T.A. Albright, J.K. Burdett, M.H. Whangbo, Orbital Interactions in Chemistry, Wiley, New York, 1985.

[17] S.D. Robinson, G. Wilkinson, J. Chem. Soc. A (1966) 300.

[18] M.A. Bennett, A.K. Smith, J. Chem. Soc. Dalton Trans. (1974) 233.

[19] W.K. Anderson, D.K. Dalvie, J. Heterocycl. Chem. 30 (1993) 1533.

[20] G.C. van Stein, G. van Koten, H. Passenier, O. Steinbach, K. Vrieze, Inorg. Chim. Acta 89 (1984) 79.

[21] C. Mealli, D.M. Proserpio, J. Chem. Ed. 67 (1990) 399.

[22] S. Alvarez, Tables of Parameters for Extended Hückel Calculations, Departamento de Quimica Inorganica, Universitàt de Barcelona, Barcelona, Spain, 1989.

[23] teXsan for Windows 1.0.1, Molecular Structure Corporation, Rigaku company, 3200 Research Forest Drive The Woodlands, TX 77381-4238, USA, 1997.

[24] G.M. Sheldrick, Acta Crystallogr. A46 (1990) 467.

[25] G.M. Sheldrick, Program for the Refinement of Crystal Structures, University of Göttingen, Göttingen, Germany, 1998.

[26] Interactive Molecular Graphics, release 5.1, Bruker AXS, Inc., Madison, WI 53719, USA, 1998.

[27] SHELXTL 5.1, Bruker AXS, Inc. 1997.